Interpretation of Wide-Angle Reflection Travel-Times in Realistic Crust-Mantle Structures

D. Bamford

Department of Geophysics, University of Edinburgh, James Clerk Maxwell Building, Mayfield Road, Edinburgh EH9 3JZ, Great Britain

Abstract. A method for the interpretation of wide-angle reflection travel-times in laterally varying crust-mantle structures is formulated. A datum correction is first carried out by ray-tracing to remove the effects of refraction above the reflector. The resulting time-distance data may be then expressed in a form which permits, given multiple coverage of the sub-surface, the independent determination of velocity and reflector topography.

The method has been tested on model data and found to be effective.

Key words: Explosion seismology – Wide-angle reflections – Lateral variations.

1. Introduction

Wide-angle reflections (WAR) from intra- and sub-crustal horizons are now routinely observed in high-resolution explosion seismic studies. The review of such studies in central Europe, edited by Giese, Stein and Prodehl (1976), contains many excellent examples and indeed, in this author's experience (Bamford et al., 1976; Bamford, 1973, 1977), wide-angle reflections from the Moho ($P_M P$) are observed more consistently than the corresponding head-wave (P_n).

It is unfortunate therefore that the problem of the interpretation of WAR travel-times in realistic, that is laterally varying, structures has received relatively little attention. Apart from the various techniques used by Russian workers (e.g. Pavlenkova, 1973) and trial-and-error approaches based on ray-tracing (Červený et al., 1974; Clee et al., 1974), few methods are available, certainly nothing to compare with the time-term approach for the interpretation of *refraction* travel-times (Willmore and Bancroft, 1960; Bamford, 1971, 1973, 1976, 1977). In this paper I suggest a comparable technique for the interpretation of WAR travel-times.

2. WAR Time-Distance Relationships

WAR time-distance relationships become rather complex in realistic structures. The well known $T^2 - X^2$ relationship for reflections is strictly applicable only in the case of a single plane horizontal reflector with uniform velocity above. In a multi-

layer situation, refraction effects cause the $T^2 - X^2$ relationship to be approximately true only close to normal incidence. Towards critical and larger angles, the time-distance relationships for a multi-plane-horizontal-layer structure can be derived as follows (Brown, 1969; Robinson, 1970):

The subsurface is specified by n homogeneous layers (numbered 1 to n from the surface), the ith layer having velocity v_i and thickness z_i. A ray leaves the surface at an angle θ_1 to the vertical, traverses the n layers, is reflected at the bottom of the nth layer and re-traverses the n layers, eventually emerging at the surface at a distance $X(n, \theta_1)$ from its starting point, where

$$X(n, \theta_1) = 2 \sin \theta_1 \sum_{i=1}^{n} z_i v_i / S_i, \tag{1}$$

with a travel-time of $T(n, \theta_1)$ where

$$T(n, \theta_1) = 2 v_1 \sum_{i=1}^{n} z_i / (v_i S_i), \tag{2}$$

where

$$S_i = [v_1^2 - (v_i \sin \theta_1)^2]^{\frac{1}{2}}.$$

From (1) and (2), T and X are related by a series expansion, the first three terms of which are

$$T(\tau_0, X) \simeq \tau_0 [1 + \tfrac{1}{2}(X/\tau_0 \sqrt{\overline{v^2}})^2 - \tfrac{1}{8}(\overline{v^4}/\overline{v^2}^2)(X/\tau_0 \sqrt{\overline{v^2}})^4 + \text{etc.}]. \tag{3}$$

The mth power of velocity is a function of $\tau_0 (\equiv T(n, 0))$, the two-way normal incidence reflection time) given by

$$\overline{v^m(\tau_0)} = (2/\tau_0) \sum_{i=1}^{n} z_i v_i^{m-1} \tag{4}$$

the τ_0 notation having been omitted in (3) for simplicity.

In the simple $T^2 - X^2$ relationship, the term containing the velocity information (X^2/v^2) is *independent* from the τ_0^2 term and hence $1/v^2$ and τ_0^2 can be estimated independently from a $T^2 - X^2$ plot. In contrast, the coefficients of the series expansion for the simplest multi-layer case involve complex velocity/layer thickness relationships ((3) and (4)). If variable dip on interfaces and inhomogeneity within layers is considered, ray-path equations analogous to (1) and (2) can be generated but any resulting $T - X$ expansion would certainly *not* be suitable for independent determination of velocity and layer thickness.

In summary, the effects of refraction in a realistic multi-layer situation can be dealt with by ray-tracing (Červený et al., 1974). However these effects frustrate attempts to partition surface-to-surface WAR travel-times for the independent determination of velocities and depths as may be achieved in the simple $T^2 - X^2$ case.

This problem can be overcome by correcting the surface-to-surface times to a horizontal datum within the layer immediately above the reflector. $T^2 - X^2$ methods can then be applied to the datum-datum travel-times. In practice this
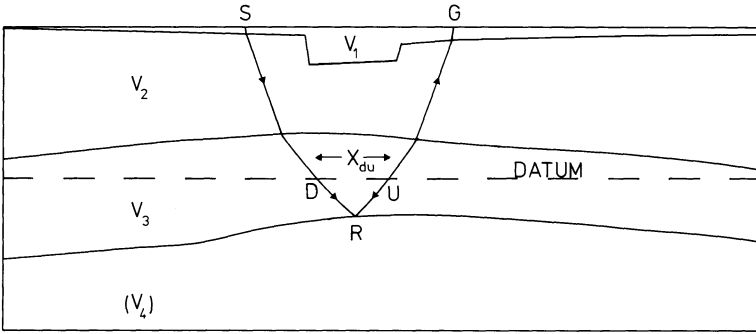
Fig. 1. Reflection, and datum correction, in a multi-layer structure
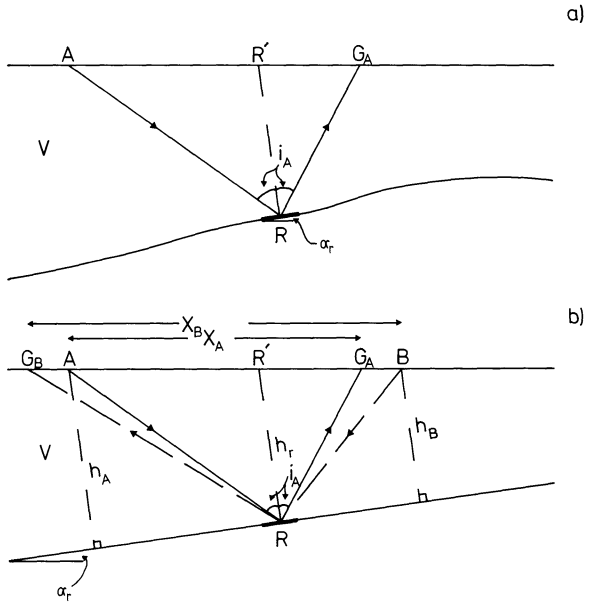

Fig. 2a and b. Reflecting element R in reflector of variable topography (a), and corresponding plane-dipping layer situation (b)

involves having reliable information on structures above the datum and a preliminary idea of those below it. A particular surface-to-surface reflection may then be ray-traced through the model so as to obtain the surface-datum and datum-surface travel-times, and the horizontal offset along the datum. Thus (Fig. 1) a reflection at R with surface-to-surface travel-time T_{SG} has a datum-datum travel-time T_r given by

$$T_r = T_{SG} - t_d - t_u$$

where t_d and t_u are the surface-datum and datum-surface travel-times respectively. The horizontal offset along the datum is X_{du} and the problem has been reduced to that of defining the relationship between T_r and X_{du} in the case of a single reflector of variable topography.

In Figure 2a, a small reflecting element R with dip α_r forms part of a reflector of variable topography, with uniform velocity V above. Reflection travel-times from

R depend only on R — reflector topography elsewhere has no effect — and so only the equivalent plane-dipping layer (Fig. 2b), for which time-distance relationships are available (e.g. Heiland, 1940, p. 262), need be considered.

The *up-dip* travel-time T_A between A and G_A is given by

$$V^2 T_A^2 = X_A^2 + 4h_A^2 - 4h_A X_A \sin \alpha_r. \tag{5}$$

If the normal from R cuts AG_A at R' $(h_r = R'R)$, then *for small dips*, $AR' = X_A/2$ and

$$h_A = h_r + \frac{X_A}{2} \sin \alpha_r$$

and, inserting this into (5), eventually

$$T_A^2 = \frac{4h_r^2}{V^2} + \frac{X_A^2 \cos^2 \alpha_r}{V^2}.$$

Likewise, the *down-dip* travel-time T_B from B to G_B is given by

$$V^2 T_B^2 = X_B^2 + 4h_B^2 + 4h_B X_B \sin \alpha_r,$$

$$h_B = h_r - \frac{X_B}{2} \sin \alpha_r$$

and

$$T_B^2 = \frac{4h_r^2}{V^2} + \frac{X_B^2 \cos^2 \alpha_r}{V^2}.$$

Thus, for small dips, the datum-datum travel-times for a reflection from R are independent of the dip direction and take the form

$$T_r^2 = \tau_r^2 + \frac{X_{du}^2 \cos^2 \alpha_r}{V^2} \tag{6}$$

with $\tau_r = \frac{2h_r}{V}$, the normal incidence reflection time.

For the kth datum-datum observation from R, (6) may be re-written as

$$T_{rk}^2 = \tau_r^2 + \frac{X_{rk}^2 \cos^2 \alpha_r}{V^2}.$$

After ray-tracing to determine the datum-datum $T-X$ data the α_r appropriate to the reflection point may be estimated from the starting model and used to form

$$D_{rk} = X_{rk} \cos \alpha_r$$

leaving T_{rk} and D_{rk} related by

$$T_{rk}^2 = \tau_r^2 + \frac{D_{rk}^2}{V^2}.$$

In this equation, the terms involving reflector topography are separated from those involving velocity and several analytical approaches are possible for their independent determination.

However, before considering these various approaches, it is necessary to consider the significance of the assumption of small dip. It is assumed that

$$AR' = R'G_A = \frac{X_A}{2}$$

whereas in fact

$$AR' = \frac{h_r \sin i_A}{\cos(i_A + \alpha_r)} \quad \text{and} \quad R'G_A = \frac{h_r \sin i_A}{\cos(i_A - \alpha_r)}$$

i.e. $\dfrac{AR'}{R'G_A} = \dfrac{\cos(i_A - \alpha_r)}{\cos(i_A + \alpha_r)}$, a ratio which tends to one when the angle of incidence (i_A) is very much greater than the dip angle (α_r), a condition that will often be fulfilled by wide-angle reflections. If the ratio $AR'/R'G_A$ does depart significantly from one, additional second-order corrections must be made to the D_{rk} values to compensate. This ratio can be examined and, if necessary, the appropriate corrections calculated during the ray-tracing stage. Thus, although the models to be discussed later contain only shallow dips and do not require these second-order corrections to be made, the assumption of small dip is not in fact necessary for the following analytical approaches to be applicable.

3. Travel-Time Analysis

The degree of multi-fold coverage necessary for the application of a separate velocity determination for every common reflection point is rarely available in crust/mantle studies. Hence accurate velocity determinations will be possible only if observations from several reflection points are combined. In practice the common reflection elements for the datum-datum reflections will be apparent only after ray-tracing and the method of combining them will depend on the degree of coverage available.

(a) *Pairs of Observations*

If two observations are available at each reflecting element, then the corresponding time-distance relationships are

$$T_{r1}^2 = \tau_r^2 + \frac{D_{r1}^2}{V^2},$$

$$T_{r2}^2 = \tau_r^2 + \frac{D_{r2}^2}{V^2}.$$

By *subtraction*

$$\Delta T_r^2 = T_{r1}^2 - T_{r2}^2 = \frac{1}{V^2}(D_{r1}^2 - D_{r2}^2) = \frac{1}{V^2}\Delta D_r^2$$

and thus a plot of ΔT_r^2 against ΔD_r^2 for all available reflection elements yields a straight line of slope $\dfrac{1}{V^2}$.

By *addition*

$$\tau_r^2 = \frac{1}{2}\left[T_{r1}^2 + T_{r2}^2 - \frac{1}{V^2}(D_{r1}^2 + D_{r2}^2)\right]$$

for each reflector element.

Some parallels with the "plus-minus" refraction interpretation method (Hagedoorn, 1959) will be recognized.

(b) Multiple Observations

If the rth reflector element has $N(r)$ reflections associated with it $(N(r) \geq 2)$ and there are M such elements, the family of theoretical time-distance equations is summarized by

$$t_{rn}^2 = \tau_r^2 + \frac{D_{rn}^2}{V^2} \tag{7}$$

where $r = 1, \text{----}, M$ (and $n = 1, \text{----}, N(r)$ for any r). Estimates of $\dfrac{1}{V^2}$ and every τ_r^2 result from forming from the observations T_{rn} and D_{rn} the sum of squared residuals I, where

$$I = \sum_{r=1}^{M} \sum_{n=1}^{N(r)} (T_{rn}^2 - t_{rn}^2)^2,$$

and reducing I to a minimum by setting

$$\frac{\delta I}{\delta\left(\dfrac{1}{V^2}\right)} = 0 \quad \text{and} \quad \frac{\delta I}{\delta(\tau_r^2)} = 0 \quad (r = 1, \text{----}, M).$$

This gives

$$\left.\begin{array}{l} \tau_r^2 = A_r - \dfrac{1}{V^2} B_r \\[2mm] \text{where} \\[2mm] A_r = \dfrac{1}{N(r)} \displaystyle\sum_{n=1}^{N(r)} T_{rn}^2 \quad \text{and} \quad B_r = \dfrac{1}{N(r)} \displaystyle\sum_{n=1}^{N(r)} D_{rn}^2 \end{array}\right\} \quad r = 1, \text{----}, M$$

and

$$V^2 = \frac{\displaystyle\sum_{r=1}^{M} \sum_{n=1}^{N(r)} (D_{rn}^2 - B_{rn})^2}{\displaystyle\sum_{r=1}^{M} \sum_{n=1}^{N(r)} (T_n^2 - A_{rn})(D_{rn}^2 - B_{rn})}$$

and also allows simple estimation of uncertainties.

The above formulation is similar to that in the time-term approach and a further parallel is that just as refractor velocity can be allowed to vary in that method (e.g. with direction; Bamford, 1973, 1976, 1977), the velocity in Equation (7) need not be uniform. Thus a small vertical velocity gradient above the reflector could be represented by

$$V^2 = V_0^2 + k D_{rn}^2 \quad (k D_{rn}^2 \ll V_0^2)$$

leading to

$$t_{rn}^2 = \tau_r^2 + \frac{D_{rn}^2}{V_0^2} - \frac{k}{V_0^4} D_{rn}^4.$$

(c) Resumé

Problems of surface-to-surface WAR travel-time interpretation can be reduced to $T^2 - D^2$ space by ray-tracing and correction to a datum. The degree of reflection coverage then controls the way in which both the velocity below the datum and the reflector topography can be independently determined.

This is an Iterative Process. The initial guess at structure below the datum can, after the first solution, be replaced by computed values, the iteration then continuing until a stable structure is achieved.

4. Model Studies

The approach described in 2. and 3. above has been tested on both model and real data. The interpretation of data from the 1974 LISPB seismic experiment (Bamford et al., 1976) will be presented elsewhere. Here the results of tests carried out on the model situation shown in Figure 3 are considered.

The crust-mantle model (Fig. 3a) incorporates a fault-bounded sedimentary basin underlain by a regionally uplifted intra-crustal interface and Moho. In the observation scheme (Fig. 3b) stations are placed every $2\frac{1}{2}$ kms along the 220 kms long recording profile, for the shotpoints shown. Theoretical Moho reflection ($P_M P$) travel-times computed by raytracing for observations in the distance range 80 to 220 kms are made more realistic by the introduction of random errors drawn from a population with zero mean, 0.1 secs standard deviation.

The sub-surface coverage offered by this observation scheme (Fig. 3b) varies from two-to five-fold, permitting both analytic approaches (3. above) to be tested. Common reflecting elements average approximately 1 km in length.

(a) Observation Pairs

Three of the several suitable groupings are considered here. These are (Fig. 3b)

> pair E, shots $E1$ and $E2$ (180/230 kms),
> pair C, shots $C1$ and $C2$ (230/270 kms),
> and pair W, shots $W1$ and $W2$ (270/320 kms),
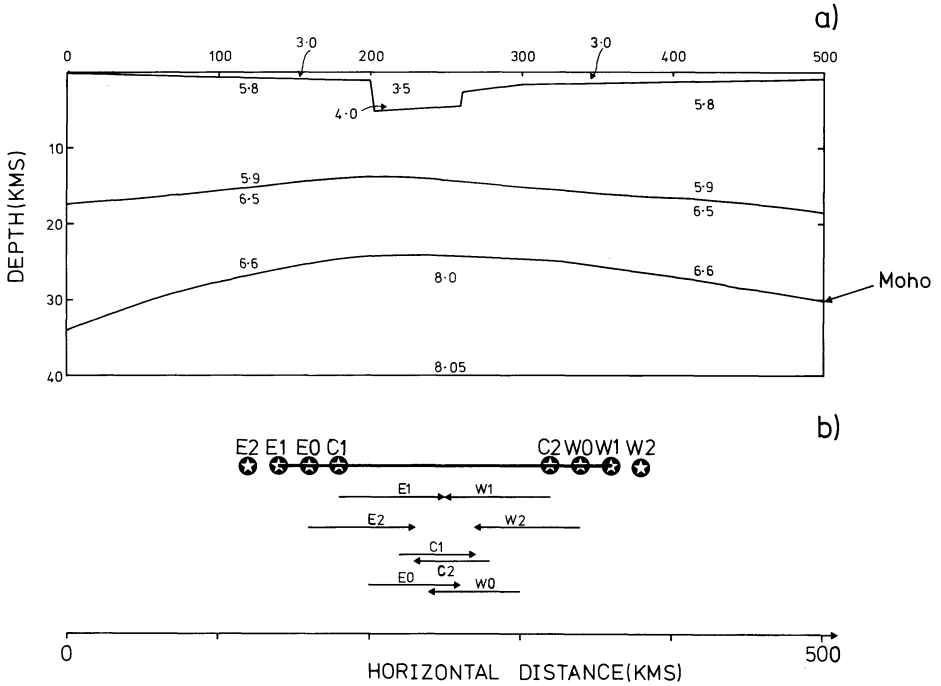
Fig. 3. a Model crust-mantle structure (velocities in km/s), and b hypothetical observation scheme and sub-surface coverage for Moho reflections. *KEY:* ⊙ shotpoint; ——— recording profile (stations every $2\frac{1}{2}$ kms); $\xrightarrow{E2}$ sub-surface coverage for each shotpoint

the figures in brackets indicating the horizontal position in the model of the corresponding sub-surface coverage.

The datum is at 20 kms depth. The structure above is assumed to be known exactly, the velocity of the layer immediately above Moho is assumed to be 6.5 km/s throughout (as compared to the actual increase from 6.5 to 6.6 km/s with depth) and to start the iteration Moho depth is assumed to be 30 kms everywhere: thus in the first iteration the dip is assumed to be zero.

After ray-tracing and datum correction, the following velocities result

pair E 6.63 ± 0.05 km/s,

pair C 6.58 ± 0.02 km/s,

pair W 6.65 ± 0.06 km/s.

The estimate for pair C is close to the actual root-mean-square value of 6.57 km/s for wide-angle reflections through the structure whereas those for pairs E and W are slightly too high. This demonstrates an important point. Equation (6)

$$T_r^2 = \tau_r^2 + \frac{X_{du}^2 \cos^2 \alpha_r}{V^2}$$
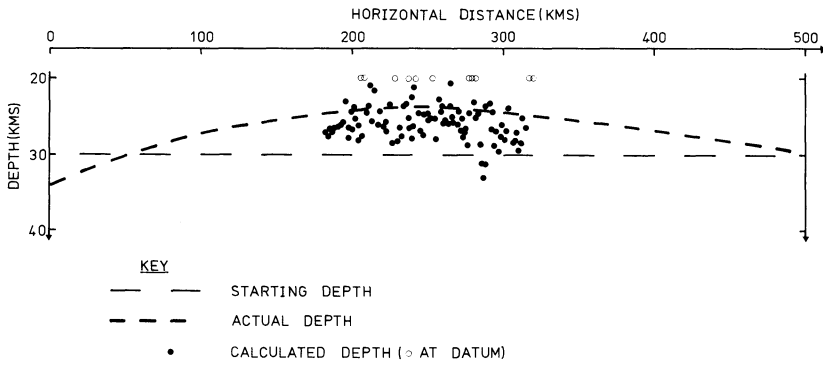
Fig. 4. Depths computed after third iteration of pairs analysis; in comparison with starting and actual models. Occasionally, a zero (or even negative) datum-corrected travel-time may result if the corresponding (introduced) random error happens to have a relatively large value. A zero (or negative) depth may then be computed — for convenience, all such values are shown as lying at the datum depth

is independent of the dip direction, and hence it seems unimportant whether the observation pairs consist of two up-dip, two down-dip or one up-dip and one down-dip observations. However, if the dip estimate in the model is in error then $D_r (= X_{du} \cos \alpha_r)$ will be also. If both observations are made with increasing distance up-dip (pairs E and W) then, for both, the error in D_r increases as the depth (i.e. τ_r) decreases and the velocity will be overestimated. On the other hand, if distance increases up-dip for one observation and down-dip for the other (pair C), then the error in D_r increases as τ_r decreases in one direction but as τ_r increases in the other. The net result will be a balance and a correct velocity calculation. This effect is likely to disappear the closer the actual model is approached and thus after the 3rd iteration, these velocities result

   pair E 6.60 $\pm$ 0.04 km/s,

   pair C 6.59 $\pm$ 0.03 km/s,

   pair W 6.60 $\pm$ 0.07 km/s

with the depths shown in Figure 4.

   Clearly the computed reflector position has moved considerably from the starting assumption towards the actual position. However, there is considerable scatter on the depths and the velocity uncertainty is rather large, and this is common to all other observation pairs considered (e.g. $E0$ and $E1$, $E1$ and $C2$). The problem is that the combination of only observation pairs does not take full advantage of the statistical improvements actually offered by the multiple coverage available. One important consequence of this is that progress towards a final model tends to be slow, and thus three more iterations were required before the structure stabilized correctly.
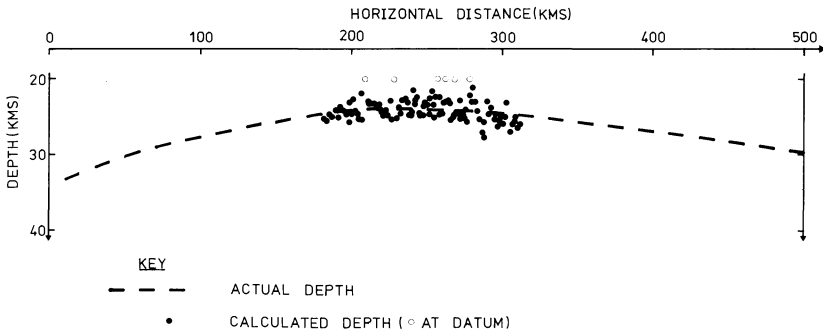
Fig. 5. Depths computed after simultaneous analysis of all data; in comparison with actual model

(b) Multiple Observations

The analytical approach defined for multiple observations allows the simultaneous use of all available travel-times (Fig. 3b). To facilitate comparisons with the analysis of observation pairs, the same starting model was used as for the 3rd iteration in the pairs analysis.

The uniform and increasing velocity options can be compared via their solution variances. In addition, any travel-time that generates an excessive residual (larger than three standard deviations) may be regarded as systematically inconsistent and removed. The resulting "clean" data give variances of 3.24 $(sec^2)^2$ and 3.25 $(sec^2)^2$ for the uniform and increasing velocity cases respectively. Thus, in the presence of introduced errors (0.1 secs. standard deviation), the slight velocity gradient above the Moho cannot be detected and the uniform velocity estimate of 6.58 ± 0.01 km/s is preferred. The resulting depth profile is shown in Figure 5; the original reflector topography has been recovered. In comparison with the analysis of pairs, this approach is rather more effective, only one iteration being required and this resulting in a better velocity estimate and less scatter of depths (Figs. 4, 5).

5. Error Propagation

A particular problem with this method is that it concentrates any error that arises anywhere on the whole travel-path into the final set of data, the datum-datum time-distance values. Thus in the foregoing model studies the measurement errors built into the travel-times eventually show up in the final stage of modelling, for example as scatter in the Moho depth estimates (Fig. 5).

In real problems, there will be two main sources of such errors:

(i) Travel-time measurement errors. Even relatively modest errors (0.1 secs standard deviation) can induce considerable scatter into the final model (Fig. 5) and so a great effort must be put into obtaining accurate initial travel-time measurements for these secondary arrivals.

(ii) Errors due to inaccuracies in the starting model. It has been found in tests that errors in the starting model *below* datum are not especially serious – they simply slow down the iterative process. However, errors in the model *above* datum will always generate similar errors in the final model below datum. In particular, systematic inaccuracies above datum will tend to skew deeper results. Further tests show that the normal random uncertainties in the velocities and depths computed in seismic studies (a few per cent) are acceptable limits for the starting model.

Other sources of error relate mainly to a failure of the assumptions of the method. In fact, there are few such assumptions. The assumption of small dip for example is one that leads to particularly simple arithmetic but it is not a necessary one. The same is true for the assumption of uniform velocity; velocity anisotropy, for example, believed to be present in the lower crust/upper mantle (Bamford, 1977) can be introduced via extra terms in Equation (6).

6. Conclusion

Model studies, and experience with real data, indicate that given multicoverage of the reflector of interest and reliable knowledge of structure above it, the approaches described can be used to interpret surface-to-surface WAR travel-times in laterally varying structures. Of the two approaches for the analysis of datum-datum times, the analysis of observation pairs with common reflection points is the simplest to carry out but the simultaneous analysis of all multi-coverage data is ultimately the most effective. A rational interpretation procedure for real problems is to begin with an approximation to the reflector topography (e.g. from refraction interpretation), iterate quickly through several pairs analyses so as to move reasonably close to the actual structure and then carry out one or two simultaneous solutions for final models.

Finally, although the concept of *reversed* profiles is of no ultimate significance in WAR studies, the combination of up- with down-dip observations does yield more reliable models in the early stages of iteration and hence quicker progress toward final models.

References

Bamford, D.: An interpretation of first-arrival data from the Continental Margin Refraction Experiment, Geophys. J. **24**, 213–229, 1971
Bamford, D.: Refraction data in Western Germany – a time-term interpretation. Z. Geophys. **39**, 907–927, 1973
Bamford, D.: MOZAIC time-term analysis. Geophys. J. **44**, 433–446, 1976
Bamford, D.: P_n velocity anisotropy in a continental upper mantle. Geophys. J. **49**, 29–48, 1977
Bamford, D., Faber, S., Jacob, B., Kaminski, W., Nunn, K., Prodehl, C., Fuchs, K., King, R., Willmore, P.: A lithospheric seismic profile in Britain – I. Preliminary results. Geophys. J. **44**, 145–160, 1976
Brown, R.J.S.: Normal-moveout and velocity relations for flat and dipping beds and for long offsets. Geophysics **34**, 180–195, 1969
Červený, V., Langer, J., Pšenčik, I.: Computation of geometric spreading of seismic body waves in laterally inhomogeneous media with curved interfaces, Geophys. J. **38**, 9–20, 1974

Clee, T.E., Barr, K.G., Berry, M.J.: Fine structure of the crust near Yellowknife. Can. J. Earth. Sci. **11**, 1534–1549, 1974

Giese, P., Stein, A., Prodehl, C. (editors): Explosion seismology in central Europe – Data and Results, 429 p. Berlin-Heidelberg-New York: Springer-Verlag, 1976

Hagedoorn, J.G.: The plus-minus method of interpreting seismic refraction sections. Geophys. Prospecting **7**, 158–182, 1959

Heiland, C.A.: Geophysical exploration, 1013 p. New York: Prentice-Hall, 1940

Pavlenkova, N.I.: Interpretation of refracted waves by the reduced travel-time curve method. Phys. Solid Earth **8**, 544–550, 1973

Robinson, J.C.: An investigation of the relative accuracy of the most common normal-moveout expressions in velocity analyses. Geophys. Prospect. **18**, 352–363, 1970

Willmore, P.L., Bancroft, A.M.: The time-term approach to refraction seismology. Geophys. J. **3**, 419–432, 1960